Changes to Intestinal Transport Physiology and Carbonate Production at Various CO_2 Levels in a Marine Teleost, the Gulf Toadfish (*Opsanus beta*)

Rachael M. Heuer[1,*]
Kathleen M. Munley[2]
Nafis Narsinghani[1]
Jessica A. Wingar[1]
Theresa Mackey[1]
Martin Grosell[1]
[1]Marine Biology and Ecology Department, Rosenstiel School of Marine and Atmospheric Science, University of Miami, 4600 Rickenbacker Causeway, Miami, Florida 33149;
[2]Department of Biological Sciences, Louisiana State University, 214 Life Sciences Building, Baton Rouge, Louisiana 70803

Accepted 6/23/2016; Electronically Published 8/11/2016

ABSTRACT

Most marine teleosts defend blood pH during high CO_2 exposure by sustaining elevated levels of HCO_3^- in body fluids. In contrast to the gill, where measures are taken to achieve net base retention, elevated CO_2 leads to base loss in the intestine of marine teleosts studied to date. This loss is thought to occur through transport pathways previously demonstrated to be involved with routine osmoregulation in marine teleosts. The main objective of this study was to characterize the intestinal transport physiology of the gulf toadfish (*Opsanus beta*) when exposed to varied levels of CO_2: control, 5,000, 10,000, and 20,000 μatm CO_2 (0.04, 0.5, 1, and 2 kPa, respectively). Results of this study suggest that intestinal apical anion exchange is highly responsive to hypercarbia, evidenced by a dose-dependent increase in intestinal luminal HCO_3^- (mmol L^{-1}) that was mirrored by a reduction in Cl^- (mmol L^{-1}). Despite activation of HCO_3^- transport pathways typically used during osmoregulation, fractional fluid absorption was only significantly lower at the highest level of CO_2. Although increased HCO_3^- excretion could provide more substrate for intestinally produced carbonates, carbonate production was not significantly increased during hypercarbia at the levels tested. This study is among the first to thoroughly characterize how compensation for elevated CO_2 affects transport physiology and carbonate production in the marine fish intestine. This deeper understanding may be particularly relevant when considering the impacts of future predicted ocean acidification, where prolonged base loss may alter the energetic cost of acid-base balance or osmoregulation in marine fish.

Keywords: hypercapnia, carbon dioxide, hypercarbia, anion exchange, fish, osmoregulation, acid-base balance, HCO_3^-, temperature, carbonate.

Introduction

The typical acid-base regulatory response exhibited by fish exposed to elevated ambient CO_2 (hypercarbia) has been well characterized across a wide array of species and exposure levels (Heisler 1984; Larsen and Jensen 1997; Claiborne et al. 2002; Evans et al. 2005; Perry and Gilmour 2006; Brauner and Baker 2009). After experiencing an initial drop in blood plasma pH and increase in pCO_2 at the onset of CO_2 exposure, most fish respond by elevating and maintaining high levels of plasma HCO_3^-. This compensation leads to an altered steady state, where pH is maintained at preexposure levels but both HCO_3^- and pCO_2 remain elevated (Toews et al. 1983; Larsen and Jensen 1997; Ishimatsu et al. 2004; Michaelidis et al. 2007; Perry et al. 2010; Esbaugh et al. 2012, 2015; Ern and Esbaugh 2016). The gill is the primary organ used to cope with elevated CO_2 and is estimated to account for ~90% of dynamic acid-base regulation in fishes (Claiborne et al 2002; Perry and Gilmour 2006). In most instances, the accumulation of HCO_3^- in the plasma is usually associated with a corresponding and equimolar decrease in plasma Cl^- (Larsen and Jensen 1997; Claiborne et al. 2002; Brauner and Baker 2009).

In addition to the gill, the intestine may also contribute to whole-body acid-base balance (Wood et al. 1999; Perry and Gilmour 2006). Most evidence to date does not suggest that the intestine dynamically regulates acid-base disturbances (Perry et al. 2010). However, the intestine is known to be responsive to changes in plasma HCO_3^- (Taylor et al. 2010; Heuer et al. 2012) and appears to counteract measures employed at the gill to retain HCO_3^- during elevated CO_2, at least during short-term exposures (Perry et al. 2010; Heuer et al. 2012). In addition, hypercarbia has recently been demonstrated to prolong specific dynamic action (Tirsgaard et al. 2015). Most patterns of acid and base flux in the intestine have been studied in the context of osmoregulation by manipulating environmental salinity (Genz et al. 2008; Scott et al. 2008; Sattin et al. 2010; Taylor et al. 2010; Guffey et al.

*Corresponding author; e-mail: rheuer@rsmas.miami.edu.

Physiological and Biochemical Zoology 89(5):402–416. 2016. 1522-2152/2016/8905-5135$15.00. DOI: 10.1086/688235

2011; Gilmour et al. 2012), since this organ is critical for osmotic homeostasis.

The link between the exchange of acid-base equivalents and osmoregulation lies in processes related to solute-coupled water absorption in the intestine. To stay hydrated, marine fish drink seawater and absorb monovalent ions (Na^+ and Cl^-), which ultimately drives water from the lumen into the body (Smith 1930; Skadhauge 1974; Usher et al. 1991). In part, Cl^- absorption occurs in exchange for HCO_3^- on the apical membrane, connecting base secretion to water absorption (Grosell and Genz 2006; Grosell et al. 2009*b*). One source of HCO_3^- for this exchange results from Na^+-coupled HCO_3^- movement from the blood to the intracellular space via the basolateral $Na^+:HCO_3^-$ cotransporter NBC1 (Taylor et al. 2010). Elevated pCO_2 also provides a source of HCO_3^- for apical anion exchange, since it is a substrate for hydration via intracellular carbonic anhydrase (CAc; Wilson et al. 1996; Grosell and Genz 2006; Sattin et al. 2010). Thus, elevated CO_2 may increase HCO_3^- secretion through increased transepithelial HCO_3^- movement via NBC1 or through increased hydration of intracellular pCO_2. Furthermore, changes to cellular Na^+ gradients that occur as a result of an increase in transepithelial HCO_3^- movement during elevated CO_2 could potentially alter the Na^+K^+ATPase (NKA), leading to increased O_2 consumption and therefore metabolic CO_2 production, providing yet another substrate for anion exchange following intracellular hydration.

A short-term study (3 d) exposing toadfish to elevated CO_2 levels relevant for global climate change scenarios predicted for year 2300 (1,900 μatm CO_2; Meehl et al. 2007) showed a significant increase in rectal base secretion that corresponded to a significant decrease in intestinal Cl^- (mmol L^{-1}), suggesting that movement through apical anion exchanger slc26a6 was increased (Heuer et al. 2012). Elevated total CO_2 in the intestinal fluid of plainfin midshipman (*Porichthys notatus*) exposed to a much higher level of CO_2 (50,000 μatm CO_2) demonstrated similar results, generally indicating that compensation for CO_2 induces base loss in the intestine that would act against measures taken at the gill to retain HCO_3^- (Perry et al. 2010). In adult medaka (*Oryzias latipes*) exposed to 7,000 μatm CO_2 for 48 h, changes in mRNA levels of transporters involved in acid secretion (NHE3), HCO_3^- regulation (NBCa, NBCb, AE1a, CA15), and various NKA subunits were noted in the intestine (Tseng et al. 2013). In contrast, NBC, NKCC2, and CAc mRNA expression did not change in the red drum (*Sciaenops ocellatus*) following exposure to 1,000 μatm CO_2 for 14 d, suggesting species-specific or exposure-level differences. However, increased branchial NKA activity and transient changes to intestinal NKCC2 mRNA expression at an earlier time point (72 h) suggested some degree of impact to osmoregulatory processes to even low levels of CO_2 exposure. (Esbaugh et al. 2015). Together, these studies indicate that compensation for elevated CO_2 elicits the use of transporters and proteins that are integral in maintaining water balance.

In addition to aiding solute coupled water uptake via anion exchange, HCO_3^- secreted into the lumen reacts with Ca^{2+} to form $CaCO_3$ to lower luminal osmotic pressure and favor continued osmotic water absorption (Grosell et al. 2009*b*; Whittamore et al. 2010). Thus, hypercarbia has been previously hypothesized to increase the production of carbonates. This hypothesis was not supported in a study on toadfish (1,900 μatm CO_2; Heuer et al. 2012); however, in the midshipmen, exposure to 50,000 μatm CO_2 for 48 h increased carbonate titratable alkalinity (TA; Perry et al. 2010). It is unclear whether differences among these studies are due to exposure level, species specificity, or a combination of both factors.

Hypercarbia may also affect carbonate composition. As fish drink seawater and monovalent ions and water are absorbed, divalent ions such as Mg^{2+}, Ca^{2+}, and SO_4^{2-} are concentrated since they are relatively impermeable to the intestinal epithelia (Marshall and Grosell 2006; Genz et al. 2008). In addition to Ca^{2+}, carbonates are also composed of Mg^{2+}, so alterations to fluid absorption could potentially change conditions for $CaCO_3$ precipitation in the intestinal lumen. While the precipitate Mg^{2+} content and thus solubility in seawater have been assessed for a wide variety of species (Perry et al. 2011; Salter et al. 2012), only one study on the toadfish has examined changes to carbonate composition with CO_2 exposure (Heuer et al. 2012). This endpoint was not significantly different at 1,900 μatm CO_2; however, it is unclear whether higher CO_2 levels would alter the composition.

Although the gill is rightfully well studied as the dominant organ responsible for regulating acid-base disturbances during hypercarbia in marine teleosts, it is nonetheless surprising that the intestine has received relatively little attention, since the secretion of HCO_3^- through the intestine appears to be linked to digestion, osmoregulation, and acid-base balance in the multifunctional gut of marine teleosts. While some information is available on how the marine fish intestine responds to hypercarbia (Perry et al. 2010; Heuer et al. 2012; Tseng et al. 2013; Esbaugh et al. 2015; Tirsgaard et al. 2015), most in vivo work on transport mechanisms is restricted to two species that were investigated at two CO_2 tensions that differ by 25-fold. The abundant gulf toadfish has served as a model for study of the marine fish intestine and more specifically for investigation of bicarbonate secretory pathways, anchoring findings from this study to a rich body of previous literature. The functional significance of these pathways in the face of salinity challenge and during digestion has been explored and is present in other species, but mechanisms underlying intestinal responses to elevated ambient CO_2 are not well documented. Understanding these responses is especially important, since it appears that in at least some circumstances, transport pathways impacted during exposure to high CO_2 may be at odds with osmoregulatory needs. Although levels in this particular study are beyond climate change–projected scenarios, results from this study could provide insight into potential physiological consequences to be investigated at lower CO_2 levels, as even small sustained perturbations to elevated CO_2 could affect energetic allocations that could manifest in population-level and ecological consequences. On this background, the overarching goal of this study was to better characterize intestinal transport mechanisms in response to hypercarbia and to explore these findings in the context of whole-body acid-base balance. To achieve these goals, we capitalized on the strength of a dose-dependent study design, examining intestinal responses in the gulf toadfish exposed to a

range of CO_2 levels (control, 5,000, 10,000, and 20,000 μatm CO_2). Our first prediction was that increased plasma HCO_3^- and pCO_2 that occur in the blood plasma during hypercarbia would lead to an increase in HCO_3^- secretion in the intestine of the toadfish. This change in intestinal transport was also expected to alter the content of other ions involved in the HCO_3^- transport pathway and support the idea that apical anion exchange is impacted by hypercarbia. Given the important role of HCO_3^- secretion in osmoregulation, the activation of this same pathway during hypercarbia was expected to potentially alter fluid transport and increase carbonate production. These predictions were tested using rectal collection sacs to examine the effect of hypercarbia on the relationship between blood acid-base chemistry and intestinal base secretion (series 1), ion concentrations in plasma and intestinal fluid (series 2), and intestinal fluid movement, base secretion rates, and carbonate composition (series 3). An additional objective was to validate the use of rectal collection sacs by examining production of carbonates collected directly from the intestine and to examine the potential for dissolution in released carbonates during elevated CO_2 exposure (series 4).

Methods

Animal Collection and Care

Gulf toadfish (*Opsanus beta*) were obtained as bycatch from shrimp fishermen in Biscayne Bay, Florida, and transported to the University of Miami Rosenstiel School of Marine and Atmospheric Science. On arrival, toadfish were treated for ectoparasites (McDonald et al. 2007) and placed into aerated tanks with flow-through seawater from Bear Cut, Florida (22°–27°C, 30–35 ppt). Polyvinylchloride tubing was provided as shelter, and all fish were acclimated to the lab for at least 2 wk before experimentation. Fish were fed squid biweekly, but food was withheld for at least 2 or 3 d before experimentation to prevent variation associated with specific dynamic action (Taylor and Grosell 2009). All protocols adhered to University of Miami animal care protocols (IACUC 13-3225).

Seawater CO_2 Manipulation

Desired pCO_2 levels were attained using a pH-stat CO_2 dosing system by Loligo Systems (Tjele, Denmark) as described in previous studies (Esbaugh et al. 2012; Heuer et al. 2012). This system utilized pH as a proxy for pCO_2 levels after a standard curve was generated by measuring pH at known CO_2-air gas mixes and ambient seawater pH. For experiments, a pH setpoint corresponding to each desired pCO_2 level was calculated, and 100% CO_2 was dosed directly into flow-through aerated tanks to achieve the chosen pCO_2 level. The pH electrode and meter (Sentix H electrode, 3310 pH meter, WTW) corresponding to each experimental tank were connected to CapCTRL software that dosed CO_2 using solenoid valves controlled by a pCO_2/pH DAQ-M digital relay instrument (Loligo Systems). Desired pCO_2 levels remained stable using this system and typically stayed within 4%–10% of setpoint values. Independent pH_{NBS} (National Bureau of Standards) of experimental tanks was validated on most days during each experimental run using an independent electrode (PHC3005, Radiometer). A Corning 965 CO_2 Analyzer (Corning Diagnostics) was used to further validate that desired CO_2 levels were being achieved. Total CO_2 readings and pH_{NBS} measurements were put into CO2SYS software to define all the other parameters of the carbonate system (pCO_2 and TA; Pierrot et al. 2006). These results, along with measurements of temperature and salinity, are presented in table A1.

Rectal Collection Sac and Blood-Sampling Protocols (Series 1–3)

Rectal collection sacs were utilized to examine the effect of hypercarbia on the relationship between blood acid-base chemistry and intestinal base secretion (series 1), ion concentrations in plasma and intestinal fluid (series 2), and intestinal fluid movement, base secretion rates, and carbonate composition (series 3). Before surgery, individual toadfish were placed into plastic containers with multiple openings to allow for water movement and submerged directly into experimental tank bottoms at their respective CO_2 level (control, ~400, 5,000, 10,000, and 20,000 μatm CO_2) for a 3-d acclimation period. The addition of submerged water pumps ensured even mixing in the tank and also facilitated water movement through the plastic containers in which the fish were kept. Fish mass was generally close to 60 g for rectal collection sac experiments (control: 66.9 $\pm$ 4.2 g; 5,000 μatm: 60.8 $\pm$ 7.6 g; 10,000 μatm: 57.2 $\pm$ 4.1 g; 20,000 μatm: 63.3 $\pm$ 4.9 g). Following this acclimation period, toadfish were anesthetized (0.2 g L^{-1} MS-222 buffered with 0.3 g L^{-1} $NaHCO_3$), and surgery was performed to attach a rectal collection sac. This sac was made from the tip of a nitrile glove attached to a 1-cm segment of a 1-mL disposable plastic syringe that was heat flared at both ends (Genz et al. 2008). Rectal collection sacs were held in place by suture stitched around the rectal opening. Thus, intestinal secretions over a time period could be collected and kept isolated from seawater. After surgery, toadfish were submerged and recovered in their respective treatment tanks, where they remained for another 3 d.

Following a total 6-d exposure (3-d acclimation, 3-d post-surgery), toadfish were anesthetized with MS-222 in ~1.5 L^{-1} of their respective treatment seawater (0.2 g L^{-1} MS-222 buffered with 0.3 g L^{-1} $NaHCO_3$). This process took around 1 min. A blood sample was drawn from the caudal vein into a heparinized syringe and immediately centrifuged to separate red blood cells and the plasma. A hemostat was used to isolate rectal collection sac contents, after which the spinal cord was severed. Plasma was measured for pH (PHC3005, Radiometer), total CO_2 (Corning 965, Corning Diagnostics), and osmolality (Wescor Vapro 5520, Logan, UT), and an aliquot of the plasma sample was frozen (−20°C) for later ion analyses. Fish were then dissected, and the intestinal tract was removed after clamping the pyloric and rectal sphincter with hemostats. All excretions (fluid and carbonate) from the rectal collection sac and samples from the intestinal tract were combined into one sample (preweighed 15-mL conical tube) for subsequent analysis.

After the final mass of conical tubes was weighed to determine total intestinal output, tubes were centrifuged (3,000 rpm for 10 min) to separate fluid and solid (carbonate) components. Fluid from the collection was isolated and weighed to determine total fluid volume and measured for pH, total CO_2, and osmolality. An aliquot of the sample was frozen (−20°C) for later ion analyses. For both plasma and rectal fluid, bicarbonate equivalents were calculated from measurements of total CO_2 and pH using the Henderson-Hasselbalch equation as outlined in a previous study (Genz et al. 2008).

Double endpoint titrations were used to analyze the total bicarbonate/carbonate equivalents in the solid carbonate portion of the rectal sample. The sample was first suspended in 10 mL of nanopure water, sonicated (Kontes micro-ultrasonic cell disrupter), and recentrifuged (see above). This procedure was repeated with new nanopure water in order to rinse the precipitates of any residual intestinal fluid that could potentially contaminate the sample. Following the second rinse, nanopure water was removed and replaced by 10 mL of 150 mmol L^{-1} NaCl and sonicated a final time. This 150 mmol L^{-1} NaCl solution was used to stabilize pH electrode readings. Before titration, the sample was gassed with N_2 for a period of 15 min, and an initial pH reading was determined (PHC 3005-8, Radiometer Analytical). N_2 gassing continued throughout the analysis. Samples were titrated with 0.2 mol L^{-1} HCl until a stable pH reading was obtained below 3.8 and then returned to the initial pH using 0.02 mol L^{-1} NaOH (British Drug Houses Standard for both acid and base, Anachemia Canada). Acid and base additions were performed using 2-mL microburettes (GS-1200, Gilmont Instruments). Total bicarbonate and carbonate equivalents were determined by subtracting the amount of NaOH from the amount of HCl used during the titration. After titration, samples were frozen (−20°C) for further ion analysis.

Ion concentrations of cations in plasma (Na^+, Mg^{2+}, Ca^{2+}), rectal fluid (Na^+, Mg^{2+}, Ca^{2+}), and rectal solid (Mg^{2+}, Ca^{2+}) carbonates were measured using flame atomic absorption spectrometry with an air/acetylene flame (Varian, Palo Alto, CA). For anions, HCO_3^- in plasma and rectal fluid was estimated using methods described above, while Cl^- (plasma and rectal fluid) and SO_4^{2-} (rectal fluid) were analyzed using anion chromatography (Dionex 120, Sunnyvale, CA).

Total rectal base secretion rate (μmol kg^{-1} h^{-1}; series 3) was determined by adding molar amounts of HCO_3^- equivalents in fluid and solid carbonates. Since temperature affects carbonate precipitation rates in the intestine (Wilson et al. 2009), carbonate production rates were normalized to 25°C by acclimating toadfish to various temperature levels and determining a correction factor (see series 5 below). Finally, drinking rate was estimated using an average of Mg^{2+} and SO_4^{2-} based estimates of drinking rates as previously described (Genz et al. 2008). Drinking rate was calculated by multiplying the rectal fluid excretion rate (mL^{-1} kg^{-1} h^{-1}) by the Mg^{2+} content (mmol L^{-1}) in rectal fluid and dividing this value by Mg^{2+} content (50 mmol L^{-1}) in seawater. The same procedure was performed for SO_4^{2-}, using a value of 30 mmol L^{-1} in seawater. The fraction of fluid absorbed was calculated by subtracting the rectal fluid excretion rate from the drinking rate and dividing this value by the drinking rate.

Series 4: Effect of Hypercarbia on $CaCO_3$ Collected Directly from Intestinal Tract and from Tank Bottom

Direct collection of carbonates from the intestinal tract of undisturbed toadfish was performed to substantiate findings from carbonate production rates in rectal collection sacs in toadfish that underwent surgery. In addition, concurrent collection of carbonates from the tank bottom in this series of the experiment allowed for direct comparison of collection methodologies and, as it turns out, dissolution of excreted $CaCO_3$. Toadfish were exposed to control (ambient), 10,000, or 20,000 μatm CO_2 for 6 d. On day 3, all carbonates and other debris were removed from the tank bottom, so that carbonates could be collected on day 6 to determine a carbonate production rate. On day 6, toadfish were sacrificed, and intestinal carbonates were collected and placed into a conical tube. To increase resolution, the carbonates from three fish from each 20-L tank were pooled for intestinal and tank bottom measurements. The average mass (g) per fish was 54.0 ± 2.0, 54.4 ± 2.0, and 53.7 ± 1.4 for control, 10,000, and 20,000 μatm CO_2 treatments, respectively. Immediately following dissections, carbonates on the bottom of each tank were collected. Double endpoint titrations were performed on samples as outlined above.

Series 5: Effects of Temperature on Carbonate Production

During the experimental period, ambient temperatures varied more than expected (22°–27°C). To test the effects of temperature on toadfish carbonate production rates, toadfish were exposed to target temperatures of 21°, 25°, 28°, and 31°C (see fig. 7 for measured values) for a total of 4 or 5 d. The first portion of the exposure (2.5–3.5 d) served as an acclimation period. All carbonates were cleared from the tank bottom following acclimation, and the next 1.5 d (42.9 ± 0.3 h) served as the collection period for carbonate production rate measurements. All fish were removed at the end of this period, and carbonates were collected from the tank bottom. Toadfish were pooled at a density of three to five per tank in this portion of the experiment when appropriate. The average mass (g) in each tank for each treatment was 43.4 ± 2.5, 46.7 ± 5.1, 41.7 ± 4.6, and 79.1 ± 20.3 for 21°, 25°, 28°, and 31°C, respectively. All other analytical procedures were as outlined in series 4. Results from this series were used to normalize all carbonate excretion rates from series 1–3.

Data Analysis

All values are reported as mean ± SEM. Since all comparisons involved at least two treatment groups in addition to a control group, one-way ANOVAs were used for all statistical comparisons, followed by Holm-Sidak tests for multiple comparisons when appropriate. Data that were not normally distributed were tested using the nonparametric Kruskal-Wallace ANOVA on ranks test followed by Dunn's method for multiple comparisons. For tem-

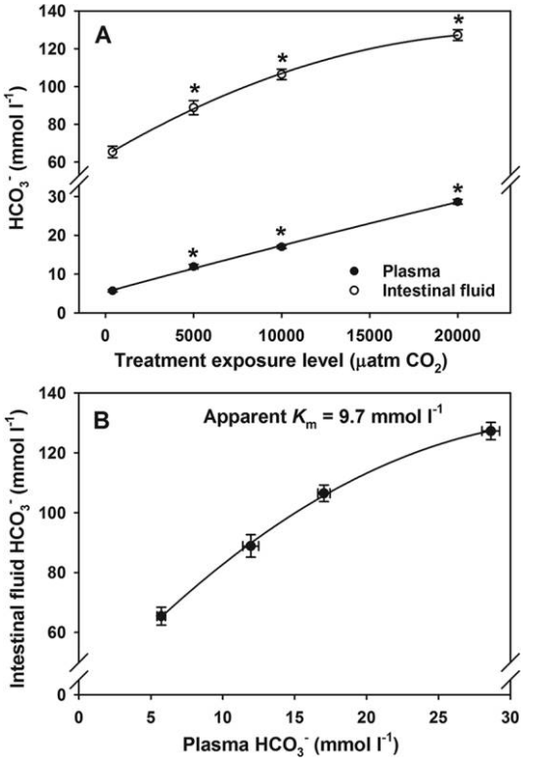

Figure 1. Relationship between CO_2 exposure level, plasma HCO_3^- (mmol L^{-1}), and intestinal fluid HCO_3^- (mmol L^{-1}). *A*, Plasma HCO_3^- and intestinal fluid HCO_3^- (mmol^{-1}) of gulf toadfish following 6 d of exposure to control (~400 μatm CO_2), 5,000, 10,000, and 20,000 μatm CO_2 (n = 17, 13, 13, 14 for plasma and n = 13, 8, 9, 11 for intestinal fluid, respectively). The HCO_3^- concentration (mmol L^{-1}) of intestinal fluid was determined from excretions collected in rectal sacs affixed on day 3 of the acclimation period and sampled on day 6. *B*, Intestinal HCO_3^- (mmol L^{-1}) as a function of plasma HCO_3^- (mmol L^{-1}). Values are mean ± SEM. An asterisk denotes a statistically significant difference from control values ($P < 0.05$).

perature data, any follow-up tests were conducted using pairwise comparisons. Significant difference was determined from controls for all tests at $P < 0.05$.

Results

Series 1: Relationship between Blood Acid-Base Chemistry and Intestinal Base Secretion

Plasma HCO_3^- exhibited a steady increase as a function of increased CO_2 levels (linear fit, $f = 0.0012x + 5.6152$, $r^2 = 0.99$), while intestinal fluid HCO_3^- (mmol L^{-1}) started to show signs of saturation at higher levels of CO_2 (quadratic polynomial fit, $f = 63.55 + 0.0055x + -1.16\text{e-}7x^2$, $r^2 = 0.99$; fig. 1*A*). A fivefold increase in plasma HCO_3^- from 400 to 20,000 μatm CO_2 translated to around a twofold increase in HCO_3^- (mmol L^{-1}) in intestinal fluids (fig. 1*A*). When intestinal fluid HCO_3^- was expressed as a function of plasma HCO_3^- (mmol^{-1}; fig. 1*B*), a quadratic polynomial fit best described the relationship ($f = 37.34 + 5.29x + -0.075x^2$, $r^2 = 0.99$).

Series 2: Effects of Hypercarbia on Ion Concentrations in Plasma and Intestinal Fluid

Similar to previous studies, the decrease in plasma Cl^- (27.9 mmol L^{-1}) appeared to be nearly equimolar to the increase in plasma HCO_3^- (22.9 mmol L^{-1}) when comparing control values to the highest CO_2 exposure level (20,000 μatm CO_2). Hypercarbia did not significantly alter Na^+, Mg^{2+}, or Ca^{2+} plasma concentration (mmol L^{-1}; fig. 2; table A2). Plasma osmolality generally declined with increasing levels of hypercarbia (one-way ANOVA, $P > 0.032$; table 1); however, post hoc tests revealed a significant decrease only at the 10,000 μatm CO_2 exposure level.

A significant increase in intestinal fluid HCO_3^- (mmol^{-1}) at all CO_2 levels occurred with a corresponding decline in Cl^- (mmol^{-1}; significant at 10,000 and 20,000 μatm CO_2; fig. 3*A*; table A2). This change was not equimolar as seen for the plasma, and the ratio of HCO_3^- increase to Cl^- decrease dropped as pCO_2 levels increased. Na^+ (mmol^{-1}) exhibited a slight increase with increasing exposure level that was not statistically significant (fig. 3*A*). Outside of a transient nonsignificant increase in SO_4^{2-} at 5,000 μatm CO_2, all three divalent ions showed a significant decrease with increasing levels of CO_2 exposure (fig. 3*B*). A trend for a decrease in intestinal fluid osmolality was also evident, although this change was not statistically significant (table 1).

Series 3: Effects of Hypercarbia on Intestinal Fluid Movement, Base Secretion Rate, and Carbonate Composition

Both the drinking rate and the rectal fluid excretion rate did not change with CO_2 exposure (fig. 4). In contrast, the fraction of fluid absorbed from imbibed seawater was significantly lower at 20,000 μatm CO_2 (fig. 4).

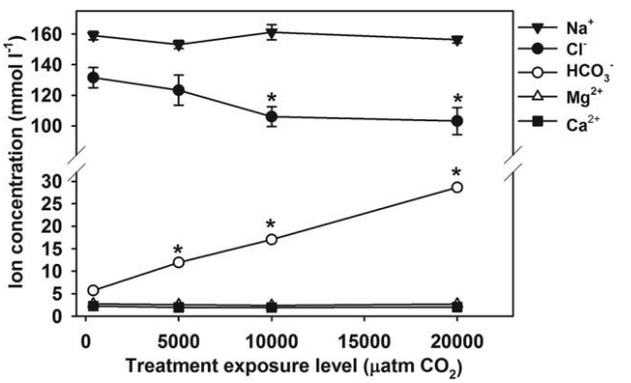

Figure 2. Plasma ion concentrations (mmol^{-1}) of toadfish exposed to various CO_2 levels. Ion concentrations (mmol L^{-1}) in plasma from gulf toadfish following 6 d of exposure to control (~400 μatm CO_2), 5,000, 10,000, and 20,000 μatm CO_2 (n = 18, 12, 12, 15 for Na^+, Ca^{2+}, and Mg^{2+}, n = 17, 13, 13, 14 for HCO_3^-, and n = 18, 9, 12, 14 for Cl^-, respectively). Samples were taken from fish that had a rectal collection sac affixed on day 3 of the exposure period. Note that HCO_3^- (mmol L^{-1}) is reported in both figures 1 and 2. Values are mean ± SEM. An asterisk denotes a statistically significant difference from control values ($P < 0.05$). Values are also shown in table A2.

Table 1: Osmolality and pH from intestinal fluid and plasma of gulf toadfish (*Opsanus beta*) exposed to various CO_2 levels

	Intestinal fluid		Plasma	
CO_2 level (μatm CO_2)	mOsm	pH	mOsm	pH
Control	330.7 ± 5.8 (13)	8.50 ± .02 (13)	314.2 ± 2.5 (18)	7.60 ± .03 (17)
5,000	327.2 ± 8.0 (8)	8.44 ± .03 (8)	312.1 ± 2.1 (12)	7.66 ± .02 (13)
10,000	321.3 ± 10.0 (9)	8.48 ± .02 (9)	304.3 ± 2.8 (13)*	7.73 ± .01 (13)*
20,000	316.0 ± 4.4 (11)	8.31 ± .02 (11)*	307.5 ± 2.3 (15)	7.74 ± .01 (14)*

Note. Osmolality (mOsm) and pH in blood plasma of mixed venous nature and intestinal fluid of gulf toadfish exposed to control (~400 μatm CO_2), 5,000, 10,000, and 20,000 μatm CO_2 for 6 d. Measurements of intestinal fluid were determined from the fluid component of excretions collected in rectal sacs affixed on day 3 of the acclimation period and collected on day 6. Values are mean ± SEM, with n in parentheses.

* Statistical significance from control values ($P < 0.05$).

Similar to findings at lower CO_2 levels, the fluid base secretion rate and the total (fluid combined with solid $CaCO_3$) base secretion rate were significantly increased with CO_2 exposure (fig. 5). The solid, or $CaCO_3$, base secretion did not change with CO_2 exposure. Consequently, the fluid component of the base secretion became an increasing proportion of the total base secretion at increasing levels of CO_2 exposure.

It is important to note that there was some variation in ambient water temperatures, generally ranging between 22° and 27°C, throughout the rectal collection sac experiments. Since temperature has been previously demonstrated to affect $CaCO_3$ precipitation rate in the sheepshead minnow (Wilson et al. 2009), the relationship between temperature and $CaCO_3$ production was estimated for the toadfish in this study (see "Series 5: Effects of Temperature on Carbonate Production" for more details; linear fit, $y = 1.6455x - 26.986$, $r^2 = 0.96$). Accordingly, solid $CaCO_3$ base secretion rates were normalized to 25°C to account for effects of inadvertent temperature variation in rectal collection sac experiments.

Ion analysis of carbonates from rectal collection sacs revealed no difference in the proportion of the $CaCO_3$ as Mg^{2+} relative to total Mg^{2+} and Ca^{2+} ions (table 2), suggesting that there were no changes in carbonate composition. The proportion of total Ca^{2+} or Mg^{2+} in the rectal sac excretion present as solid $CaCO_3$ or the intestinal fluid did not change with CO_2 exposure (table 3). These results also support the finding that the ionic composition of carbonates was not altered.

Series 4: Effect of Hypercarbia on $CaCO_3$ Collected Directly from Intestinal Tract and from Tank Bottom

To confirm that surgical procedures and the use of rectal sacs outlined above did not affect the ability to detect a change in carbonate formation in the intestine, we collected carbonates directly from undisturbed toadfish exposed to control, 10,000, or 20,000 μatm CO_2 for 6 d. Similar to findings from rectal collection sacs, these spot collections from toadfish showed a trend for an increase in carbonate production with an increase in pCO_2; however, it was not statistically significant (fig. 6*A*). In contrast to intestinal carbonate production, precipitates collected from the tank bottom were significantly reduced at 20,000 μatm CO_2 (fig. 6*B*).

Series 5: Effects of Temperature on Carbonate Production

To account for the effects of temperature on carbonate production, we collected rectal carbonates produced by toadfish over ~1.5 d (42.9 ± 0.3 h) from the tank bottom. Carbonate production rate (μmol kg^{-1} h^{-1}) increased significantly with

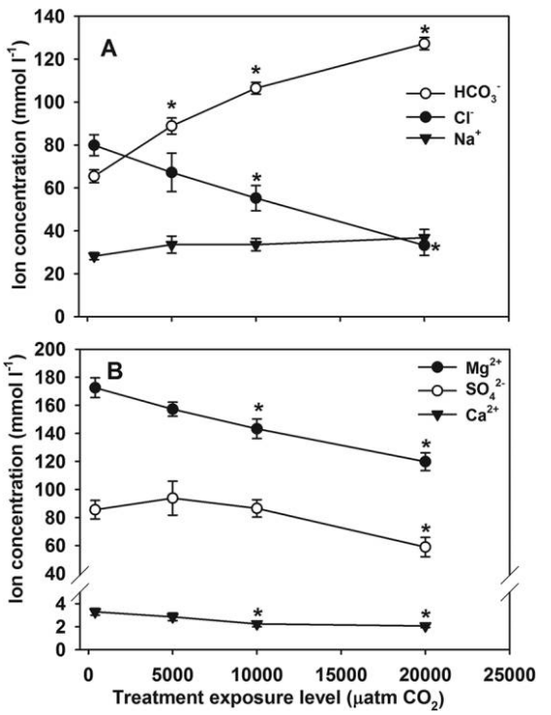

Figure 3. Intestinal fluid ion concentrations (mmol L^{-1}) of toadfish exposed to various CO_2 levels. Concentrations (mmol L^{-1}) of monovalent (*A*) and divalent (*B*) ions from intestinal fluid of gulf toadfish following 6 d of exposure to control (~400 μatm CO_2), 5,000, 10,000, and 20,000 μatm CO_2 (n = 13, 8, 9, 11, respectively). Ion concentrations of intestinal fluid were determined from excretions collected in rectal sacs affixed on day 3 of the acclimation period and sampled on day 6. Note that HCO_3^- (mmol^{-1}) is presented in both figures 1 and 3. Values are mean ± SEM. An asterisk denotes a statistically significant difference from control values ($P < 0.05$). Values are also shown in table A3.

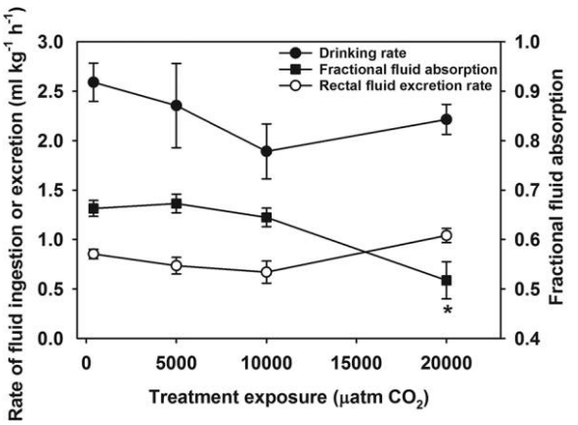

Figure 4. Drinking rate, rectal fluid excretion rate, and fraction fluid absorption of toadfish exposed to various CO_2 levels. Estimated drinking rate (mL kg^{-1} h^{-1}), rectal fluid excretion rate (mL kg^{-1} h^{-1}), and fractional fluid absorption of gulf toadfish following 6 d of exposure to control (~400 μatm CO_2), 5,000, 10,000, and 20,000 μatm CO_2 ($n = 11, 8, 9, 10$, respectively). Drinking rates were estimated using intestinal fluid Mg^{2+} and SO_4^{2+} concentrations ($mmol^{-1}$) from rectal collection sacs affixed on day 3 and sampled on day 6 of the acclimation period and also from concentrations of these ions in seawater (Genz et al. 2008). The fractional fluid absorption was calculated by dividing the fluid absorption rate by the drinking rate ((drinking rate − fluid absorption rate)/drinking rate). Values are mean ± SEM. An asterisk denotes a statistically significant difference from control values ($P < 0.05$).

increasing temperature (fig. 7; linear fit, $y = 1.6455x - 26.986$, $r^2 = 0.96$).

Discussion

As expected, exposing gulf toadfish over a range of CO_2 levels allowed for a more thorough characterization of the intestinal response to hypercarbia. Results from this study demonstrated that increased plasma HCO_3^- activated HCO_3^- transport pathways in the intestine that have previously been implicated in osmoregulation. The resulting intestinal HCO_3^- loss countered adjustments to retain HCO_3^- in the body needed to maintain and defend blood plasma pH. The stimulation of HCO_3^- transport pathways led to dilution of divalent ions in intestinal fluids with increasing CO_2 levels, suggesting potential impacts of hypercarbia on intestinal fluid absorption. Finally, despite an expectation for increased intestinal carbonate production that would theoretically scale to the observed increase in HCO_3^- secretion, there were no differences in the production of carbonates with increasing CO_2 exposure.

Like many other species, toadfish accumulate HCO_3^- to correct pH during a CO_2-induced acidosis. This linear rise in plasma HCO_3^- was dose dependent and tightly regulated, suggesting that toadfish have the capacity to cope with even higher CO_2 levels (fig. 1*A*). In contrast to the other species, toadfish appear to compensate for a CO_2-induced acidosis through HCO_3^- uptake rather than acid excretion, as fish held in nominally HCO_3^--free seawater (182 μmol L^{-1}) were unable to effectively correct pH (Esbaugh et al. 2012). While this mechanism was used by toadfish exposed to 1,900 μatm CO_2, it is unknown whether this strategy would shift to H^+ excretion with increasing CO_2 exposure. Plasma pH was significantly increased in the 10,000 and 20,000 μatm CO_2 exposures compared to controls (table 1). This trend would be opposite if compensation were incomplete, as has been noted at high levels of CO_2 in certain species, where extracellular pH is partially compensated and intracellular pH is preferentially regulated (Brauner and Baker 2009). Overall, the plasma pH values were low compared to previous measurements from cannulated toadfish (Esbaugh et al. 2012; Koldkjaer et al. 2013), as would be expected for samples obtained by caudal puncture due to pCO_2 increases in anesthetized and air-exposed fish (Esbaugh et al. 2015). It is also possible that samples from fish exposed to higher CO_2 levels, where blood pCO_2 was higher relative to ambient air, could have experienced greater CO_2 off-gassing, raising pH. Indeed, calculated pCO_2 values for plasma samples approach pCO_2 levels of the water as pCO_2 increased and was lower than ambient in fish exposed to 20,000 μatm CO_2 (data not shown). Accordingly, caution should be applied when interpreting the apparent overshoot of pH compensation. The possibility that plasma HCO_3^- levels were underestimated in samples obtained by caudal puncture due to CO_2 of gassing, especially at high CO_2 levels, is not supported by the linear increase in plasma HCO_3^-. Such HCO_3^- loss would be highest at high CO_2 concentration and would have resulted in loss of linearity at higher CO_2 levels. Though HCO_3^- accumulation in the plasma does not appear to be limited, HCO_3^- (mmol L^{-1}) in intestinal fluid may plateau (fig. 1*A*), demonstrating an upper limit to HCO_3^- secretion into the intestine. Interestingly, when intestinal HCO_3^- was plotted as a function of plasma HCO_3^-

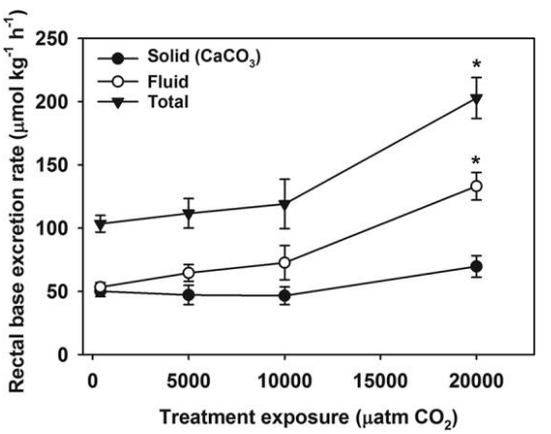

Figure 5. Rectal base secretion rates of toadfish exposed to various CO_2 levels. Rectal base excretion rates (μmol kg^{-1} h^{-1}) of gulf toadfish following 6 d of exposure to control (~400 μatm CO_2), 5,000, 10,000, and 20,000 μatm CO_2 ($n = 11, 8, 9, 10$, respectively). Ion concentrations of intestinal fluid were determined from the fluid component of excretions collected in rectal sacs affixed on day 3 of the acclimation period and collected on day 6. Total rectal base excretion is the sum of solid (carbonate) and fluid base equivalents. Values are mean ± SEM. An asterisk denotes a statistically significant difference from control values ($P < 0.05$).

Table 2: Percentage of carbonates as Mg^{2+}

CO_2 level (μatm CO_2)	%Mg
Control	50.7 ± 1.3
5,000	52.6 ± 2.8
10,000	50.5 ± 1.5
20,000	46.8 ± 1.6

Note. Percentage of whole carbonate (Ca^{2+} and Mg^{2+}) present as Mg^{2+}. Values are mean ± SEM. No statistically significant differences were noted ($P < 0.05$).

(fig. 1*B*), the calculated apparent K_m (9.7 mmol L^{-1}) was similar to that noted during in vitro isolated tissue experiments performed in a combined Ussing/pH-stat system (10.2 mmol L^{-1}) and was also similar to the K_m for HCO_3^- uptake in isolated tfNBCe1 expressed in xenopus oocytes (8.5 mmol L^{-1}; Taylor et al. 2010). This finding suggests that in vitro and in vivo transport characteristics are likely similar and lends support to the use of isolated tissue analyses to study intestinal transport mechanisms.

Similar to many previous studies (Toews et al. 1983; Larsen and Jensen 1997; Claiborne et al. 2002; Hayashi et al. 2004; Brauner and Baker 2009), the increase in plasma HCO_3^- was paired with a nearly equimolar decline in plasma Cl^-. All other ions (Na^+, Mg^{2+}, and Ca^{2+}) showed no significant differences (fig. 3). In the intestinal fluid, increased HCO_3^- (mmol L^{-1}) was mirrored by a reduction in Cl^- ($mmol^{-1}$), providing robust support to previous findings at lower CO_2 levels that exposure to CO_2 impacts apical anion exchange in the intestine (Heuer et al. 2012). This increase in HCO_3^- loss from the body counteracts whole-body acid-base balance, since the retention and/or uptake of HCO_3^- is necessary for compensation. Anion exchanger slc26a6 has been cloned in both the seawater-acclimated pufferfish (Kurita et al. 2008) and the toadfish (Grosell et al. 2009*b*) and is an electrogenic exchanger ($nHCO_3^-/Cl^-$). Results of this study comparing the concentrations of HCO_3^- and Cl^- support this assertion since exchange was not equimolar in control fish. Although it is clear that anion exchange increases drastically with CO_2 exposure in the intestine, it appears that the ratio of $\Delta HCO_3^-/\Delta Cl^-$ at each CO_2 level relative to control values declines as CO_2 exposure increases ($\Delta HCO_3^-/\Delta Cl^-$ 1.85, 1.66, and 1.33 at 5,000, 10,000, and 20,000 μatm CO_2, respectively). This change in ratios is not likely due to a shift in Cl^- uptake from slc26a6 to apical NCC or NKCC1 cotransport, since Na^+ concentrations remained stable across CO_2 levels (figs. 3, 8). Alternatively, this reduction could theoretically reflect an increase in the incorporation of HCO_3^- into $CaCO_3$ precipitates, but there was no significant change in carbonate precipitation. A third viable explanation for this observation is an increase in the activity of the recently recognized apical H^+ pump. The H^+ pump secretes H^+ into the intestinal lumen and titrates some of the secreted HCO_3^-, reducing HCO_3^- accumulation in the boundary layer and decreasing osmotic pressure, both of which are thought to facilitate continued anion exchange and water absorption during salinity stress (Grosell 2011*a*; Guffey et al. 2011) (fig. 8). Significantly lower pH in the intestinal fluid of fish exposed to the highest CO_2 level (20,000 μatm CO_2) also supports the idea of an increase in apical H^+ pump activity.

All three divalent ions (Mg^{2+}, SO_4^{2-}, Ca^{2+}) were significantly lower at higher CO_2 levels (fig. 3*B*). These ions are concentrated in the lumen as fish drink seawater, since they are relatively impermeable to absorption in the intestine. A relatively large proportion of Ca^{2+} in the rectal excretion is incorporated into the precipitation of $CaCO_3$. In isolation, a lower concentration of Ca^{2+} (mmol L^{-1}) at higher CO_2 levels would suggest an increase in precipitation. However, the lack of a significant difference in carbonate rectal output and similar patterns of decline in other divalent ions (Mg^{2+} and SO_4^{2-}) suggests that fluid transport is impacted by hypercarbia, at least at high levels of CO_2. Decreased fractional fluid absorption at 20,000 μatm CO_2 supports this assertion and is discussed below.

Neither the calculated rate of seawater ingestion (drinking rate) nor the rectal fluid excretion rate was significantly impacted by hypercarbia (fig. 4). The control of drinking is under hormonal control and is responsive to changes in plasma osmolality and external salinity (see Takei and Loretz 2011 for a detailed review). Luminal levels of Na^+ and Cl^- have also been hypothesized to control drinking rate in the Japanese eel in a feedback system where Cl^- inhibits drinking at higher luminal levels but at lower levels allows for Na^+ to stimulate drinking (Ando and Nagashima 1996). If this is the case for marine teleosts in general, the lack of change in Na^+ could explain why drinking rate was not

Table 3: Relative percent of Mg^{2+} and Ca^{2+} in intestinal fluid and $CaCO_3$ (solid) portion of excretions from rectal collection sacs

	Ca^{2+}		Mg^{2+}	
CO_2 level (μatm CO_2)	% in fluid	% in carbonate	% in fluid	% in carbonate
Control	18.0 ± 1.8	82.0 ± 1.8	91.5 ± .4	8.5 ± .4
5,000	19.4 ± 5.0	80.6 ± 5.0	90.6 ± 1.3	9.4 ± 1.3
10,000	12.5 ± 1.5	87.5 ± 1.5	89.4 ± .9	10.6 ± .9
20,000	13.0 ± 2.1	87.0 ± 2.1	89.3 ± 1.1	10.7 ± 1.1

Note. Percent of Ca^{2+} and Mg^{2+}, respectively, as fluid and solid ($CaCO_3$) component of total excretion collected from gulf toadfish exposed to control (~400 μatm CO_2), 5,000, 10,000, and 20,000 μatm CO_2 for 6 d ($n = 11, 8, 9, 10$, respectively). Measurements of intestinal fluid were determined from the fluid component of excretions collected in rectal sacs affixed on day 3 of the acclimation period and collected on day 6. Values are mean ± SEM. No statistically significant differences were noted ($P < 0.05$).

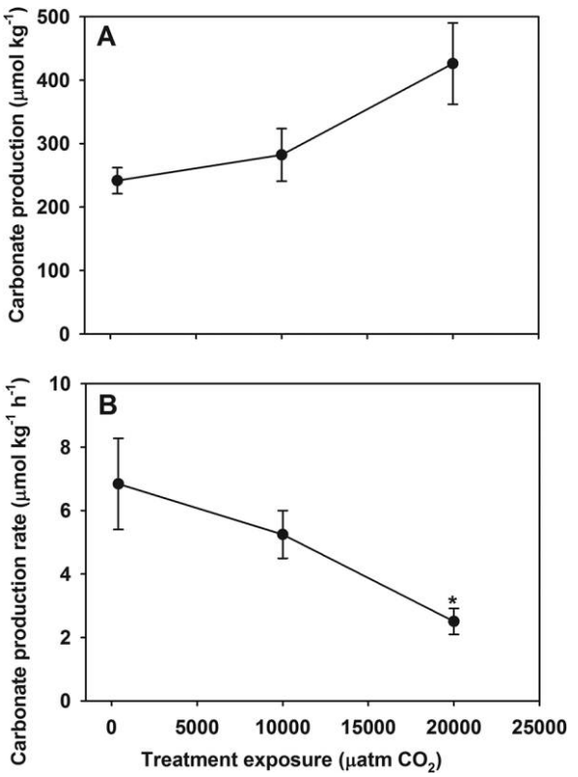

Figure 6. Carbonates found in the toadfish intestine compared to carbonate dissolution rate in tank bottom with varied CO_2 exposure. Intestinal carbonate content in *A* was determined from carbonates residing in the intestine of fish sacrificed after 6 d of exposure to control (~400 μatm CO_2), 10,000, and 20,000 μatm CO_2 ($n = 5$ groups of 3 fish). *B*, Net intestinal carbonate appearance in tanks of gulf toadfish acclimated to control (~400 μatm CO_2), 10,000, and 20,000 μatm CO_2 ($n = 5$ groups of 3 fish) for 3 d. All carbonates were cleared from the tank bottom after the first 3 d, and carbonates were collected from day 3 to day 6 to determine the carbonate production rate. Values are mean ± SEM. An asterisk denotes a statistically significant difference from control values ($P < 0.05$).

influenced by hypercarbia despite dramatic reductions in luminal Cl^- (mmol L^{-1}). Considering both the drinking rate and the rectal fluid excretion rate, we can assume an estimate of imbibed fluid that is absorbed. At the highest CO_2 level, fish did not change their drinking rate but absorbed significantly less of the imbibed fluid than control fish (fig. 4). The ultimate cause of this lowered fractional fluid absorption is unclear, especially considering there may have been a slightly more favorable osmotic gradient for water movement from the intestine to the blood. The absolute reduction in osmolality was smaller in the plasma (~Δ6 mOsm) than what was observed in the intestinal fluid (~Δ15 mOsm) at 20,000 μatm CO_2.

Similar to previous findings (Heuer et al 2012), the total and fluid rate of rectal base secretion increased with CO_2 exposure, but there was no change in the solid $CaCO_3$ base secretion rate (fig. 5), suggesting that carbonate production in the toadfish does not change even at high levels of hypercarbia. Midshipman show an increased TA of carbonates when exposed to 50,000 μatm CO_2 for 48 h (Perry et al. 2010), so it is unclear whether the lack of difference in toadfish reflects a species-specific difference or is related to the level of CO_2 exposure or ambient temperature (the midshipman study was conducted at 13°C). In addition to production rates, the composition of carbonates was unchanged with hypercarbia. It was previously hypothesized that an increase in Mg^{2+} incorporation could occur with hypercarbia if already low levels of Ca^{2+} became limiting for precipitation with an increase in carbonate production, since Mg^{2+} is typically high in luminal fluids (Heuer et al. 2012). This was clearly not the case since carbonate production did not change and divalent ions declined in a similar manner as described above. In the species studied to date, Mg^{2+} content and structure of carbonates vary considerably (Perry et al. 2011; Salter et al. 2012). Accordingly, examining both production and composition in other species during hypercarbia may be valuable.

To confirm that surgical procedures and the use of rectal sacs did not affect the ability to detect a change in carbonate formation in the intestine, we spot-collected carbonates from undisturbed toadfish exposed to control, 10,000, or 20,000 μatm CO_2 using the same exposure time as above (6 d). Carbonates collected using this alternative method also showed no significant increase in production although a trend was observed for increased presence of $CaCO_3$ precipitates in the intestinal lumen at 20,000 μatm (fig. 6*A*). In contrast, collections of carbonates from the tank bottom indicated a significant dose-dependent decrease in carbonate production that was significant at 20,000 μatm CO_2. This decrease is not due to a lack of production, since the intestinal lumen shows

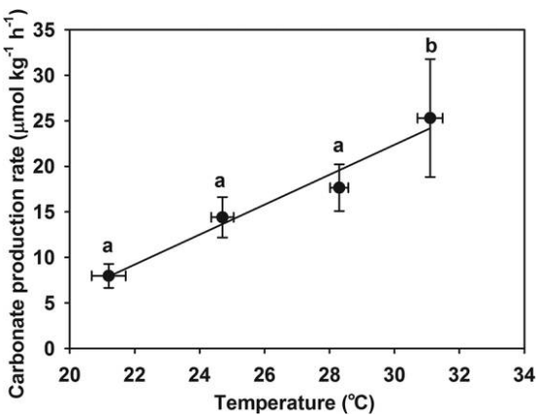

Figure 7. Effect of temperature on carbonate production rate in the gulf toadfish. Carbonate production rate (μmol kg^{-1} h^-) of gulf toadfish as a function of temperature (°C) at ambient control CO_2 (~400 μatm CO_2). Carbonate production rates were determined by performing double endpoint titrations (Genz et al. 2008) on carbonates collected from the tank bottom following ~1.5 d (42.9 ± 0.3 h) of exposure. Temperature acclimation *n* numbers were 6, 12, 12, and 4 at 21.2°, 24.7°, 24.8°, and 31.1°C, respectively. Due to the small size of some fish, carbonates from more than one fish per tank were pooled for analysis. Values are mean ± SEM. Letters represent statistically significant differences using a one-way ANOVA, followed by a pairwise multiple comparison (Holm-Sidak, $P < 0.05$). Linear fit, $y = 1.6455x - 26.986$, $r^2 = 0.96$).

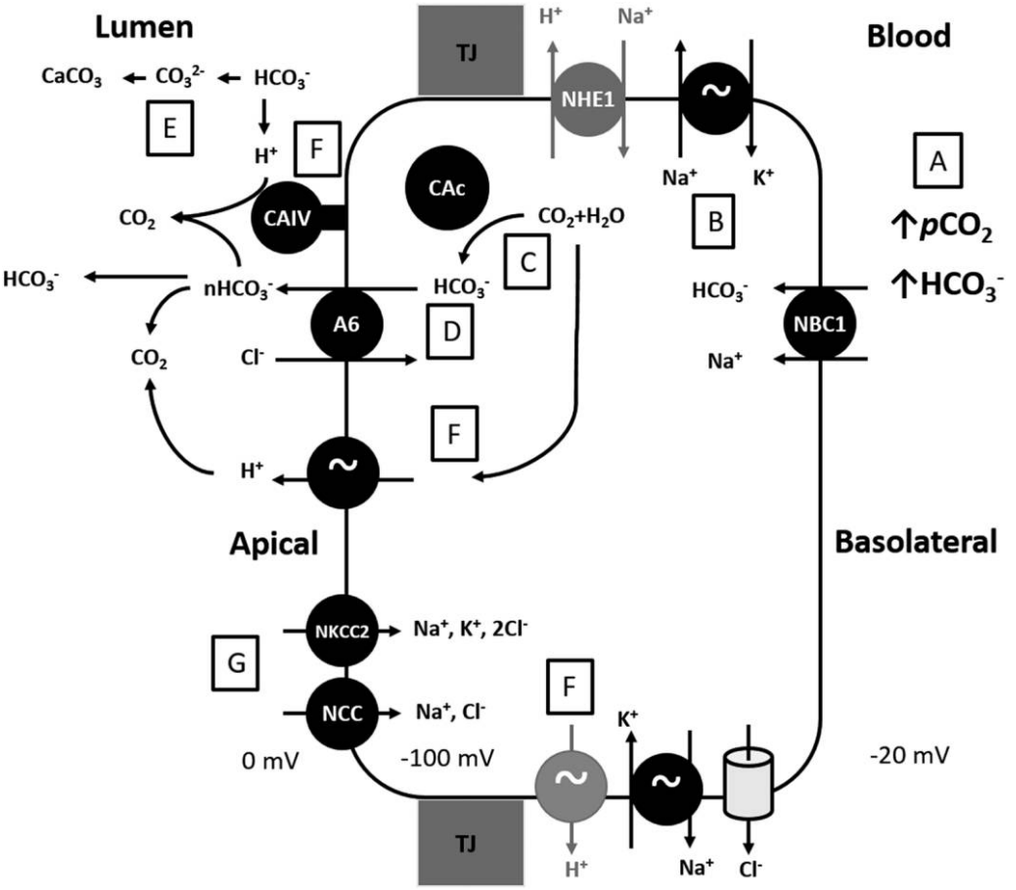

Figure 8. Proposed effects of elevated CO_2 on epithelial transport in the gulf toadfish (*Opsanus beta*). Toadfish exposed to elevated CO_2 in seawater show a tightly regulated increase of HCO_3^- in the blood plasma to defend pH. *A*, Elevation of plasma HCO_3^- likely stimulates Na^+:HCO_3^- cotransporter NBC1 (Taylor et al. 2010), increasing cytosolic levels of HCO_3^- and Na^+. *B*, Elevated cellular Na^+ influx could potentially lead to an increase in Na^+:K^+ ATPase mRNA expression and/or activity. Such an elevation would increase energetic demand, leading to an increase in O_2 consumption and metabolic intracellular CO_2 production. *C*, Resulting increased intracellular CO_2 would provide more substrate for carbonic anhydrase (CAc). Equilibration of plasma pCO_2 (*A*) with the intestinal cell provides a second avenue for increased intracellular pCO_2 available for hydration via CAc. *D*, HCO_3^- resulting from increased basolateral NBC1 transport and/or increased hydration of intracellular pCO_2 likely leaves the cell on the apical side via slc26a6 in exchange for Cl^-. Impacts to anion exchange are supported by a large increase in HCO_3^- (mmol L^{-1}) in intestinal fluid that corresponds to a large decrease in Cl^- (mmol L^{-1}) with increasing CO_2 exposure (fig. 2). Cl^- likely exits the cell through chloride channels on the basolateral membrane. *E*, Some CO_3^{2-}/HCO_3^- combines with Ca^{2+} and Mg^{2+} to form high Mg^{2+} $CaCO_3$; however, despite an increase in HCO_3^- secretion into the intestinal lumen, the production and composition of carbonates are not impacted by hypercarbia in the gulf toadfish. *F*, Protons (H^+) generated from intracellular CO_2 hydration exit the cell, in part, through apical H^+ pump (vacuolar-ATPase; Guffey et al. 2011) or potentially through Na^+-dependent extrusion. Protons secreted into the lumen may titrate some HCO_3^- through dehydration via membrane-bound carbonic anhydrase (CAIV) to form CO_2 that presumably titrates HCO_3^- and reduces luminal osmotic pressure. It is not clear whether processes in *F* would be impacted by hypercarbia. *G*, Despite increased Na^+ movement into the cell through NBC1 described in *B*, there was no change to plasma or luminal Na^+ ($mmol^{-1}$), suggesting that Na^+ uptake from the lumen into the cell via existing Na^+ transport pathways (NKCC2 and NCC) is likely not stimulated with hypercarbia. See Grosell (2011*a*, 2011*b*) for further detail on marine fish intestinal cellular transport mechanisms.

constant or perhaps even elevated carbonate levels at higher ambient pCO_2, but rather to a product of dissolution that occurred in the tank bottom due to reduced seawater pH. The low value of carbonate production (fig. 6*B*) as assessed by collection from the tank bottom compared to that found in the rectal collection sac even at control levels may suggest that some degree of dissolution in seawater occurs, even at normal seawater pH. Indeed, toadfish carbonates have been found to be 1.95 times more soluble than aragonite (Woosley et al. 2012), pointing to a likelihood of dissolution at normal pH that would be enhanced by reduced seawater pH. The pH in luminal fluids is typically well above seawater pH (8.50 in this particular study), meaning that carbonates are bathed in highly alkaline conditions before excretion. Since the solubility and structure of carbonates vary across species, the stability of carbonates after excretion may also vary. For example, highly soluble amorphous excretions

tend to undergo rapid dissolution in seawater (Foran 2013) and would likely not be a good candidate for collection from the tank bottom as a proxy for excretion rates.

As seen in another study on the sheepshead minnow (*Cyprinodon vareigatus*; Wilson et al. 2009), temperature significantly increased carbonate production from the toadfish. The calculated temperature quotient (Q_{10}) for this increase was 3.21, a value similar to previously reported Q_{10} (2.33) for carbonate production as a function of temperature in the sheepshead minnow (Wilson et al. 2009). While the mechanism underlying this relationship was not specifically addressed in this study, increased temperature is thought to elevate both baseline metabolism and drinking rate (Wilson et al. 2009). $CaCO_3$ excretion rates in rectal collection sac experiments were corrected to a single temperature (25°C) using the relationship between temperature and carbonate production. This adjustment did not change the outcome of the presented experiments significantly but likely provides a better representation of the solid carbonate production rate. It is also important to note that a higher average fish mass in the highest-temperature treatment could have influenced results.

Conclusions and Future Directions

It is clear from intestinal fluid measurements that hypercarbia leads to an increase in apical anion exchange in at least two fish species and across a wide range of CO_2 levels (1,900–20,000 μatm CO_2 in the gulf toadfish, 50,000 μatm CO_2 in the plainfin midshipmen; Perry et al. 2010; Heuer et al. 2012). Increased gene expression of AE1a in the intestine of seawater-acclimated medaka following hypercarbia exposure (7,000 μatm CO_2) also supports these findings (Tseng et al. 2013), suggesting that this response may be ubiquitous among marine teleosts. Continuous base loss through the intestine counteracts measures at the gill to attain net HCO_3^- retention and defend blood pH. The functional consequence of this sustained base loss is unclear but could result in a reallocation or increase in energetic demands on the intestine, since many transporters involved in HCO_3^- transport are secondarily active and depend on the gradients established by NKA (Grosell 2011*a*).

While impacts to anion exchange with respect to CO_2 are evident across all examined CO_2 levels, the intracellular source of this extra HCO_3^- could come from transepithelial HCO_3^- transport and/or increased intracellular CO_2 hydration (fig. 8). Interestingly, the transepithelial movement of HCO_3^- does not generate a proton. However, the hydration of intracellular CO_2 creates HCO_3^- available for apical anion exchange while concurrently producing a proton that must be eliminated from the cell to avoid intracellular acidification. Since these sources could differ in terms of the cascade effects on intestinal transport, understanding this balance may be important, especially since species already vary in their modes of Cl^- absorption. For example, the seawater-acclimated trout obtains all of its HCO_3^- for anion exchange from intracellular hydration (Grosell et al. 2009*a*), whereas the European flounder (*Platichthys flesus*) and gulf toadfish can obtain up to 50% through transepithelial HCO_3^- transport (Grosell et al. 2005; Grosell and Genz 2006).

Unlike anion exchange, carbonate production measured using two different methods (rectal collection sacs and spot sampling) does not appear to change dramatically under high CO_2, at least in the toadfish. A third method, utilizing collections from the tank bottom, illustrated that under high CO_2 levels, carbonates excreted by fish tend to undergo some degree of dissolution. In addition to production, all measures of carbonate composition, including proportionate amounts of Mg^{2+} and Ca^{2+}, exhibited no difference. Since Mg^{2+} content is often proportional with solubility (Wilson et al. 2009; Woosley et al. 2012), it is likely that carbonates do not become more soluble with CO_2 exposure, although ocean acidification could increase dissolution of carbonates regardless of Mg^{2+} content. Unlike CO_2, temperature does affect carbonate production, which is not unexpected given that elevated temperature elevates metabolic rate. While fluid absorption was lower at the highest CO_2 level, drinking rate and rectal fluid excretion rate were not altered with CO_2, indicating that hypercarbia does not stimulate an increase in fluid ingestion.

Furthermore, it is interesting that both salinity and hypercarbia result in increased intestinal HCO_3^- secretion. Hypersalinity appears to increase the production of carbonates (Genz et al. 2008), while hypercarbia does not. During hypersalinity, the concentrations of both Ca^{2+} and Mg^{2+} are significantly increased in luminal fluids. Since Ca^{2+} and Mg^{2+} were lower although not completely depleted during exposure to CO_2, the lack of increased $CaCO_3$ precipitation during hypercarbia may reflect substrate availability. The difference in responses to hypersalinity and hypercarbia is likely due to a difference in drinking rate, which is known to be increased in hypersalinity (Genz et al. 2008) but is not impacted by hypercarbia. Little is known about calcification processes in the marine fish intestine, so additional work in this area would be valuable.

Many studies have examined the basic mechanistic response of fish to CO_2 in the plasma, but less is known about intestinal responses. Carbon dioxide levels utilized in this study were admittedly high compared to what would be seen in the environment, even under the most drastic climate change scenarios (Meehl et al. 2007). However, in certain coastal and upwelling areas, CO_2 levels occasionally meet or exceed these predictions (Feely et al. 2008; Thomsen et al. 2010; Melzner et al. 2013), and fish in high-density aquaculture settings regularly experience high levels of CO_2 (Tirsgaard et al. 2015). Few studies have examined impacts of hypercarbia on osmoregulatory processes (Brauner et al. 2000; Shaughnessy et al. 2015), despite the fact that the maintenance of homeostasis involves the exchange of Na^+ and Cl^- and/or HCO_3^- and H^+. These findings pose interesting questions about bicarbonate transport pathways and their associated functional significance in the context of evolutionary processes. The impact of hypercarbia on osmoregulation is underrepresented in the recently burgeoning area of research looking at the effects of low-level hypercarbia on fish at near-future predicted CO_2 levels (Heuer and Grosell 2014), and further work in this area may aid interpretation of other downstream impacts. All investigated marine teleosts appear to secrete bicarbonate (Grosell et al. 2001; Grosell 2006; Perry

et al. 2011), meaning that any potential impacts to baseline metabolism or energetic reallocations as a consequence of sustained higher CO_2 levels expected under future CO_2 scenarios could impact ecosystems. Finally, although not demonstrated in this study, even small increases to carbonate production or alterations to carbonate composition could alter the fish contribution to the global oceanic carbon cycle.

Acknowledgments

R.M.H. is supported by a National Science Foundation (NSF) Graduate Research Fellowship (DGIE-0951782), and M.G. is supported by a NSF Award (1146695) and is a Maytag Chair of Ichthyology. N.N. received support from the Howard Hughes Institute Undergraduate Research Training Program.

APPENDIX

Table A1: Water chemistry parameters for CO_2 exposure levels and temperature experiments

Series 1–3: rectal collection sac and blood sampling						
CO_2 level (μatm CO_2)	pH (NBS)	pCO_2 (μatm)	Titratable alkalinity (μmol kg^{-1})	Total CO_2 (μmol kg^{-1})	Salinity (ppt)	Temperature (°C)
Control	8.14 ± .02	4,46.4 ± 19.9	2,387.1 ± 47.8	2,131.7 ± 40.2	34.9 ± .3	25.2 ± .8
5,000	7.21 ± .01	4,910.4 ± 70.0	2,410.6 ± 52.7	2,508.6 ± 54.7	34.8 ± .4	24.8 ± 1.1
10,000	6.92 ± .01	9,661.6 ± 243.2	2,403.1 ± 38.6	2,660.0 ± 46.1	34.7 ± .4	24.7 ± 1.1
20,000	6.62 ± .02	19,953.3 ± 487.0	2,373.7 ± 33.4	2,935.1 ± 56.6	34.9 ± .4	24.7 ± 1.1

Series 4: $CaCO_3$ collected from intestinal tract and tank bottom			
CO_2 level (μatm CO_2)	Salinity (ppt)	Temperature (°C)	pH (NBS)
Control	31.0 ± .2	26.1 ± .2	8.20 ± .04
10,000	31.0 ± .3	26.2 ± .3	7.07 ± .05
20,000	31.0 ± .2	26.0 ± .2	6.70 ± .05

Series 5: Effects of temperature on carbonate production	
Temperature (°C)	Salinity (ppt)
21.2 ± .5	34.2 ± .07
24.7 ± .3	34.3 ± .03
28.3 ± .3	34.5 ± .03
31.1 ± .4	34.2 ± .1

Note. Values are presented as mean ± SEM. NBS = National Bureau of Standards.

Table A2: Plasma ion concentrations (mmol L^{-1}) of toadfish exposed to various CO_2 levels

	Control	5,000 (μatm CO_2)	10,000 (μatm CO_2)	20,000 (μatm CO_2)
Na^+	159.0 ± 2.7	153.1 ± 2.6	161.2 ± 5.0	156.3 ± 2.2
Cl^-	131.6 ± 6.6	123.3 ± 9.8	106.0 ± 6.4*	103.2 ± 8.8*
HCO_3^-	5.7 ± .3	11.9 ± .6*	17.0 ± .4*	28.6 ± .6*
Mg^{2+}	2.7 ± .1	2.5 ± .2	2.4 ± .1	2.7 ± .2
Ca^{2+}	2.2 ± .2	2.0 ± .2	1.9 ± .2	2.0 ± .2

Note. Ion concentrations (mmol L^{-1}) in plasma from gulf toadfish following 6 d of exposure to control (~400 μatm CO_2), 5,000, 10,000, and 20,000 μatm CO_2 represented in figure 2. Values are mean ± SEM.

* Statistically significant difference from control values ($P < 0.05$).

Table A3: Intestinal fluid ion concentrations (mmol L^{-1}) of toadfish exposed to various CO_2 levels

	Control	5,000 (μatm CO_2)	10,000 (μatm CO_2)	20,000 (μatm CO_2)
Na^+	28.2 ± 1.6	33.6 ± 4.0	33.6 ± 2.8	36.8 ± 3.8
Cl^-	79.0 ± 4.8	67.2 ± 8.9	55.3 ± 5.9*	33.3 ± 4.7*
HCO_3^-	65.4 ± 3.0	88.9 ± 3.8*	106.5 ± 2.8*	127.2 ± 2.9*
Mg^{2+}	172.6 ± 7.1	157.3 ± 5.1	143.3 ± 7.0*	119.8 ± 6.3*
Ca^{2+}	3.3 ± .3	2.9 ± .3	2.2 ± .3*	2.1 ± .1*
SO_4^{2-}	85.6 ± 6.6	93.8 ± 12.1	86.5 ± 6.2	58.9 ± 6.9

Note. Ion concentrations (mmol L^{-1}) in intestinal fluid from gulf toadfish following 6 d of exposure to control (~400 μatm CO_2), 5,000, 10,000, and 20,000 μatm CO_2 represented in figure 3. Ion concentrations of intestinal fluid were determined from excretions collected in rectal sacs affixed on day 3 of the acclimation period and sampled on day 6. Values are mean ± SEM.

* Statistically significant difference from control values ($P < 0.05$).

Literature Cited

Ando M. and K. Nagashima. 1996. Intestinal Na^+ and Cl^- levels control drinking behavior in the seawater-adapted eel *Anguilla japonica*. J Exp Biol 199:711–716.

Brauner C.J. and D.W. Baker. 2009. Patterns of acid-base regulation during exposure to hypercarbia in fishes. Springer, Berlin.

Brauner C.J., M. Seidelin, S.S. Madsen, and F.B. Jensen. 2000. Effects of freshwater hyperoxia and hypercapnia and their influences on subsequent seawater transfer in Atlantic salmon (*Salmo salar*) smolts. Can J Fish Aquat Sci 57:2054–2064.

Claiborne J.B., S.L. Edwards, and A.I. Morrison-Shetlar. 2002. Acid-base regulation in fishes: cellular and molecular mechanisms. J Exp Zool 293:302–319.

Ern R. and A.J. Esbaugh. 2016. Hyperventilation and blood acid–base balance in hypercapnia exposed red drum (*Sciaenops ocellatus*). J Comp Physiol B 186:1–14.

Esbaugh A.J., R. Ern, W.M. Nordi, and A.S. Johnson. 2015. Respiratory plasticity is insufficient to alleviate blood acid-base disturbances after acclimation to ocean acidification in the estuarine red drum, *Sciaenops ocellatus*. J Comp Physiol B 186:97–109.

Esbaugh A.J., R. Heuer, and M. Grosell. 2012. Impacts of ocean acidification on respiratory gas exchange and acid-base balance in a marine teleost, *Opsanus beta*. J Comp Physiol B 182:921–934.

Evans D.H., P.M. Piermarini, and K.P. Choe. 2005. The multifunctional fish gill: dominant site of gas exchange, osmoregulation, acid-base regulation, and excretion of nitrogenous waste. Physiol Rev 85:97–177.

Feely R.A., C.L. Sabine, J.M. Hernandez-Ayon, D. Ianson, and B. Hales. 2008. Evidence for upwelling of corrosive "acidified" water onto the continental shelf. Science 320:1490–1492.

Foran E., S. Weiner, and M. Fine. 2013. Biogenic fish-gut calcium carbonate is a stable amorphous phase in the gilthead seabream, *Sparus aurata*. Sci Rep 3:1700.

Genz J., J.R. Taylor, and M. Grosell. 2008. Effects of salinity on intestinal bicarbonate secretion and compensatory regulation of acid-base balance in *Opsanus beta*. J Exp Biol 211: 2327–2335.

Gilmour K.M., S.F. Perry, A.J. Esbaugh, J. Genz, J.R. Taylor, and M. Grosell. 2012. Compensatory regulation of acid-base balance during salinity transfer in rainbow trout (*Oncorhynchus mykiss*). J Comp Physiol 182:259–274.

Grosell M. 2006. Intestinal anion exchange in marine fish osmoregulation. J Exp Biol 209:2813–2827.

———. 2011*a*. Intestinal anion exchange in marine teleosts is involved in osmoregulation and contributes to the oceanic inorganic carbon cycle. Acta Physiol 202:421–434.

———. 2011*b*. The role of the gastrointestinal tract in salt and water balance. Fish Physiol 30:135–164.

Grosell M. and J. Genz. 2006. Ouabain sensitive bicarbonate secretion and acid absorption by the marine fish intestine play a role in osmoregulation. Am J Physiol 291:R1145–R1156.

Grosell M., J. Genz, J.R. Taylor, S.F. Perry, and K.M. Gilmour. 2009*a*. The involvement of H^+-ATPase and carbonic anhydrase in intestinal HCO_3^- secretion on seawater-acclimated rainbow trout. J Exp Biol 212:1940–1948.

Grosell M., C.N. Laliberte, S. Wood, F.B. Jensen, and C.M. Wood. 2001. Intestinal HCO_3^- secretion in marine teleost fish: evidence for an apical rather than a basolateral Cl^-/HCO_3^- exchanger. Fish Physiol Biochem 24:81–95.

Grosell M., E.M. Mager, C. Williams, and J.R. Taylor. 2009*b*. High rates of HCO_3^- secretion and Cl^- absorption against adverse gradients in the marine teleost intestine: the involvement of an electrogenic anion exchanger and H^+-pump metabolon? J Exp Biol 212:1684–1696.

Grosell M., C.M. Wood, R.W. Wilson, N.R. Bury, C. Hogstrand, C. Rankin, and F.B. Jensen. 2005. Bicarbonate secretion plays a role in chloride and water absorption of the European flounder intestine. Am J Physiol 288:R936–R946.

Guffey S., A. Esbaugh, and M. Grosell. 2011. Regulation of apical H^+-ATPase activity and intestinal HCO_3^- secretion in marine fish osmoregulation. Am J Physiol 301:R1682–R1691.

Hayashi M., J. Kita, and A. Ishimatsu. 2004. Acid-base responses to lethal aquatic hypercapnia in three marine fishes. Mar Biol 144:153–160.

Heisler N. 1984. Acid-base regulation in fishes. Fish Physiol 10: 315–401.

Heuer R.M., A.J. Esbaugh, and M. Grosell. 2012. Ocean acidification leads to counterproductive intestinal base loss in the gulf toadfish (*Opsanus beta*). Physiol Biochem Zool 85:450–459.

Heuer R.M. and M. Grosell. 2014. Physiological impacts of elevated carbon dioxide and ocean acidification on fish. Am J Physiol 307:R1061–R1084.

Ishimatsu A., T. Kikkawa, M. Hayashi, K.S. Lee, and J. Kita. 2004. Effects of CO_2 on marine fish: larvae and adults. J Oceanogr 60:731–741.

Koldkjaer P., M.D. McDonald, I. Prior, and M. Berenbrink. 2013. Pronounced in vivo hemoglobin polymerization in red blood cells of gulf toadfish: a general role for hemoglobin aggregation in vertebrate hemoparasite defense? Am J Physiol 305:R1190–R1199.

Kurita Y., T. Nakada, A. Kato, H. Doi, A.C. Mistry, M.H. Chang, M.F. Romero, and S. Hirose. 2008. Identification of intestinal bicarbonate transporters involved in formation of carbonate precipitates to stimulate water absorption in marine teleost fish. Am J Physiol 294:R1402–R1412.

Larsen B.K. and F. Jensen. 1997. Influence of ionic composition on acid-base regulation in rainbow trout (*Oncorhynchus mykiss*) exposed to environmental hypercapnia. Fish Physiol Biochem 16:157–170.

Marshall W.S. and M. Grosell. 2006. Ion transport, osmoregulation and acid-base balance. Pp. 177–230 *in* D. Evans and J.B. Claiborne, eds. Physiology of fishes. 3rd ed. CRC, Boca Raton, FL.

McDonald M.D., K.M. Gilmour, J.F. Barimo, P.E. Frezza, P.J. Walsh, and S.F. Perry. 2007. Is urea pulsing in toadfish related to environmental O_2 or CO_2 levels? Comp Biochem Physiol A 146:366–374.

Meehl G.A., T.F. Stocker, W.D. Collins, P. Friedlingstein, A.T. Gaye, J.M. Gregory, A. Kitoh, et al. 2007. Global climate projections—Climate Change 2007: the physical science basis. Contribution of Working Group I to the Fourth Assessment Report of the Intergovernmental Panel on Climate Change. S. Soloman, D. Qin, M. Manning, Z. Chen, M. Marquis, K.B. Averyt, M. Tignor, and H.L. Miller, eds. Cambridge University Press, Cambridge.

Melzner F., J. Thomsen, W. Koeve, A. Oschlies, M. Gutowska, H. Bange, H. Hansen, and A. Körtzinger. 2013. Future ocean acidification will be amplified by hypoxia in coastal habitats. Mar Biol 160:1875–1888.

Michaelidis B., A. Spring, and H.O. Portner. 2007. Effects of long-term acclimation to environmental hypercapnia on extracellular acid-base status and metabolic capacity in Mediterranean fish *Sparus aurata*. Mar Biol 150:1417–1429.

Perry C.T., M.A. Salter, A.R. Harborne, S.F. Crowley, H.L. Jelks, and R.W. Wilson. 2011. Fish as major carbonate mud producers and missing components of the tropical carbonate factory. Proc Natl Acad Sci USA 108:3865–3869.

Perry S.F., M.H. Braun, J. Genz, B. Vulesevic, J. Taylor, M. Grosell, and K.M. Gilmour. 2010. Acid-base regulation in the plainfin midshipman (*Porichthys notatus*): an aglomerular marine teleost. J Comp Physiol 180:1213–1225.

Perry S.F. and K. Gilmour. 2006. Acid-base balance and CO_2 excretion in fish: unanswered questions and emerging models. Respir Physiol Neurobiol 154:199–215.

Pierrot D., E. Lewis, and D. Wallace. 2006. MS Excel program developed for CO_2 system calculations. ORNL/CDIAC-105a. Carbon Dioxide Information Analysis Center, Oak Ridge National Laboratory, US Department of Energy, Oak Ridge, TN.

Salter M.A., C.T. Perry, and R.W. Wilson. 2012. Production of mud-grade carbonates by marine fish: crystalline products and their sedimentary significance. Sedimentology 59:2172–2198.

Sattin G., M.E. Mager, and M. Grosell. 2010. Cytosolic carbonic anhydrase in the gulf toadfish is important for tolerance to hypersalinity. Comp Biochem Physiol 156:169–175.

Scott G.R., D.W. Baker, P.M. Schulte, and C.M. Wood. 2008. Physiological and molecular mechanisms of osmoregulatory plasticity in killifish after seawater transfer. J Exp Biol 211:2450–2459.

Shaughnessy C.A., D.W. Baker, C.J. Brauner, J.D. Morgan, and J.S. Bystriansky. 2015. Interaction of osmoregulatory and acid-base compensation in white sturgeon (*Acipenser transmontanus*) during exposure to aquatic hypercarbia and elevated salinity. J Exp Biol 218:2712–2719.

Skadhauge E. 1974. Coupling of transmural flows of NaCl and water in intestine of eel (*Anguilla-Anguilla*). J Exp Biol 60: 535–546.

Smith H.W. 1930. The absorption and excretion of water and salts by marine teleosts. Am J Physiol 93:480–505.

Takei Y. and C.A. Loretz. 2011. The gastrointestinal tract as an endocrine/neuroendocrine/paracrine organ: organization, chemical messengers and physiological targets. Fish Physiol 30:261–317.

Taylor J.R. and M. Grosell. 2009. The intestinal response to feeding in seawater gulf toadfish, *Opsanus beta*, includes elevated base secretion and increased epithelial oxygen consumption. J Exp Biol 212:3873–3881.

Taylor J.R., M.E. Mager, and M. Grosell. 2010. Basolateral NBCe1 plays a rate-limiting role in transepithelial intestinal HCO_3^- secretion serving marine fish osmoregulation. J Exp Biol 213:459–468.

Thomsen J., M.A. Gutowska, J. Saphörster, A. Heinemann, K. Trübenbach, J. Fietzke, C. Hiebenthal, et al. 2010. Calcifying invertebrates succeed in a naturally CO_2-rich coastal habitat but are threatened by high levels of future acidification. Biogeosciences 7:3879–3891.

Tirsgaard B., D. Moran, and J.F. Steffensen. 2015. Prolonged SDA and reduced digestive efficiency under elevated CO_2 may explain reduced growth in Atlantic cod (*Gadus morhua*). Aquat Toxicol 158:171–180.

Toews D.P., G.F. Holeton, and N. Heisler. 1983. Regulation of the acid-base status during environmental hypercapnia in the marine teleost fish *Conger conger*. J Exp Biol 107:9–20.

Tseng Y.C., M.Y. Hu, M. Stumpp, L.Y. Lin, F. Melzner, and P.P. Hwang. 2013. CO_2-driven seawater acidification differentially affects development and molecular plasticity along life history

of fish (*Oryzias latipes*). Comp Biochem Physiol A 165:1190–1130.

Usher M.L., C. Talbot, and F.B. Eddy. 1991. Intestinal water transport in juvenile Atlantic salmon (*Salmo salar* L.) during smolting and following transfer to seawater. Comp Biochem Physiol 100A:813–818.

Whittamore J.M., C.A. Cooper, and R.W. Wilson. 2010. HCO_3^- secretion and $CaCO_3$ precipitation play major roles in intestinal water absorption in marine teleost fish in vivo. Am J Physiol 298:R877–R886.

Wilson R.W., K.M. Gilmour, R.P. Henry, and C.M. Wood. 1996. Intestinal base excretion in the seawater-adapted rainbow trout: a role in acid-base balance? J Exp Biol 199:2331–2343.

Wilson R.W., F.J. Millero, J.R. Taylor, P.J. Walsh, V. Christensen, S. Jennings, and M. Grosell. 2009. Contribution of fish to the marine inorganic carbon cycle. Science 323:359–362.

Wood C.M., C.L. Milligan, and P.J. Walsh. 1999. Renal responses of trout to chronic respiratory and metabolic acidoses and metabolic alkalosis. Am J Physiol 277:R482–R492.

Woosley R.J., F.J. Millero, and M. Grosell. 2012. The solubility of fish-produced high magnesium calcite in seawater. J Geophys Res 117:C04018.